Andreev scattering of quasiparticle wave packets and current-voltage characteristics of superconducting metallic weak links

Reiner Kümmel and Uwe Gunsenheimer
Physikalisches Institut der Universität Würzburg, D-8700 Würzburg, Germany

Roberto Nicolsky
Instituto de Física, Universidade Federal do Rio de Janeiro, Caixa Postal 68528, 21945 Rio de Janeiro, Brazil
(Received 15 December 1989)

Current-voltage characteristics (CVC's) of superconductor–normal-conductor–superconductor junctions and their dependence on temperature and mean free path are calculated in a relaxation-time model for quasiparticles moving in a constant electric field between the walls of the pair potential well. By forming wave packets from the nonequilibrium electron and hole solutions of the time-dependent Bogoliubov–de Gennes equations, a detailed microscopic picture of quasiparticle acceleration and electron-hole (Andreev) scattering is obtained. Computing the time-averaged current density from these wave packets, one obtains the characteristic features of experimentally observed CVC's in microbridges, *SNS* sandwiches, and point contacts (including such with high-T_c superconductors). They are the "foot" at low voltages $V \ll \Delta/e$, negative differential conductivity, and subharmonic gap structure (SGS) for $V \leq 2\Delta/en$, $n = 1,2,3,\ldots$, and the excess current if eV is much larger than the maximum value Δ of the pair potential. Pronounced arches appear for voltages in the SGS regime, if one takes into account the weakening of Andreev reflection by normal scattering from the outer surfaces of relatively thin S layers. The theory is valid at any temperature below T_c and for any mean free path.

I. INTRODUCTION

Superconductor – normal-conductor – superconductor (*SNS*) junctions in their various shapes and structures[1,2] represent a class of superconducting weak links where Josephson-like macroscopic quantum phenomena occur that cannot be seen in the classical tunneling contacts. The low capacitance of *SNS* junctions is advantageous for certain applications of the Josephson effect.[2] Phase coherence between the superconducting banks can be maintained over much longer distances than in tunneling contacts. It is mediated by quasiparticles that move unscattered from one superconducting bank to the other. If the proximity effect creates a finite although reduced pair potential in short N layers, phase coherence is enhanced by Cooper pairs.

In wide N layers with vanishing pair potential, currents influenced by phase coherence are essentially carried by electrons and holes that are localized in the N region and generate each other periodically by Andreev scattering[3,4] in the *NS* interfaces, inducing supercurrents in the S layers. These bound electron-hole states determine the electronic properties of *SNS* junctions with sufficiently deep pair-potential wells. (Even small spatial variations of the order parameter result in electron-hole interferences that have been observed, e.g., in the Tomasch effect.[5,6]) For clean *SNS* junctions with infinite mean free path l, Ishii[7] and Bardeen and Johnson[8] have calculated the dc Josephson current carried by the spatially quantized electron-hole (Andreev) states. Svidzinsky *et al.*[9] investigated in detail the contributions from the bound and the continuum states to the Josephson current, which largely cancel each other. For finite mean free paths l of the order of the normal region thickness d ($\gg$ coherence length) Kulik and Mitsai[10] obtained the dc Josephson current proportional to $\sin\phi\exp(-l/d)$. Octavio, Skocpol, and Tinkham[11] measured current-voltage characteristics (CVC's) of tin variable-thickness microbridges at temperatures between 0.82 T_c and T_c, which exhibit a rapid rise of the current with small voltages (the so called "foot" or "shoulder") and the excess current at high voltages $V \gg 2\Delta/e$; pronounced, archlike structures with indications of negative differential conductivity (NDC) are observed at low temperatures for $V < 2\Delta/e$. After these authors had discussed the supercurrent enhancement in the light of the theories of Aslamazov, Larkin[12] and Golub[13] as a consequence of nonequilibrium quasiparticle distributions in the microbridge, Schmid, Schön, and Tinkham[14] analysed the quasiparticle dynamics in short microbridges, where the motion of the order parameter in the bridge leads to a deficit of quasiparticles bound in the pair-potential well, and thus, to an effective cooling and enhanced supercurrent. Computing nonequilibrium quasiparticle distribution functions from Boltzmann's equation as well as using the quasiclassical Green's-function approach they found the "foot" structure. For point contacts or sufficiently short microbridges Artemenko, Volkov, and Zaitsev[15] computed the excess current from the equations for the ordinary Green's functions and the Gorkov functions. In a series of papers, starting with a semiphenomenological one-dimensional "semiconductor model" that explained the "subharmonic

gap structure" (SGS) in weak links Klapwijk, Blonder, Tinkham,[16,17] and Octavio *et al.*[18] pointed out the fundamental importance of Andreev scattering for a physical understanding of the observed (positive) differential conductivities and CVC's. They also took into account a possible mismatch of the Fermi velocities in the N and S layers.[18–21] This stimulated further investigations of Andreev scattering and its influence on CVC's (Refs. 22–24) and partly motivated the attempt of this paper to give a detailed microscopic description of charge transport in *SNS* junctions based on wave-packet solutions of the Bogoliubov–de Gennes equations. The resulting theory of weak link current voltage characteristics complements the existing ones and offers a unified explanation of the principal phenomena, including the ones that have remained unexplained so far like the arches in the CVC's of microbridges and the NDC associated with the foot and the subharmonic gap structure.

In Sec. II we discuss the relaxation-time model that is a generalization of the conventional description of electron dynamics in normal-conductivity theory to inhomogeneous superconductors. The time-averaged current densities carried by accelerated, multiply Andreev reflected quasiparticle wave packets localized in the depression of the pair potential are calculated in Sec. III, and the resulting current voltage characteristics with foot, NDC, SGS, and excess current are computed in Sec. IV. A discussion of the simple physical picture that explains these phenomena by the interplay between quasiparticle energy gain from the electric field and multiple Andreev reflections under the influence of inelastic and surface scattering, a critique of the model, and comparison with experiments conclude the paper.

II. QUASIPARTICLE DYNAMICS AND THE RELAXATION TIME MODEL

There are several methods to analyze nonstationary charge transport in weak links. If one is dealing, e.g., with dirty normal metals of *SNS* bridges into which superconductivity has been induced by the proximity effect,[1] phase-slip centers in dirty superconducting filaments near T_c (Refs. 25 and 26) or short weak links[2] the time-dependent Ginzburg-Landau equations[26–28] are a powerful tool. In addition there are the Green's function and Boltzmann-equation methods.[14] If, on the other hand, one wants to avoid restrictions by temperature, mean free path, and sample dimensions and get a detailed quantum-mechanical picture of quasiparticle motion and its repercussions on the ground state, the time-dependent Bogoliubov-de Gennes equations[3,29] (BdGE) are appropriate. In order to treat our problem, they are combined with the following relaxation-time model for charge transport under the influence of an electric field and inelastic scattering.

We consider a voltage-biased *SNS* junction with a constant electric field in the N layer and negligible field penetration into the superconducting banks. We disregard all influences of possible ac voltage components that oscillating supercurrents might induce in the impedance of the external electrodynamic system. Although a perfect voltage bias should be possible only in a resonant circuit, and acceptable approximation is to shunt the sample by a resistance of optimized magnitude in order to introduce a dc voltage much larger than the amplitude of the oscillating component. This method has been used by Octavio[30] for variable thickness bridges and by Klein *et al.*[31] for the measurement of flux flow in thin superconducting films.

The physical picture of quasiparticle motion in such a junction, with an electric field in negative z direction perpendicular to the *NS* interfaces, is illustrated by the example of Fig. 1: At time $t=0$ a quasiparticle of energy E_k starts its motion in the N region from the position $z=-b$ as an electron $(-e)$; k stands for three quantum numbers that characterize an equilibrium quasiparticle state. Its momentum component in z direction, mv_z, is opposite to the electric field. Under multiple Andreev reflections[32] it climbs up the pair-potential well until it is being scattered or leaves the well and travels into the field-free superconductors as an imbalanced excitation. Each Andreev reflection (AR) is associated with the conversion of an electron into a hole $(+e)$ and vice versa and the induction of a supercurrent in the S regions.[29] Quan-

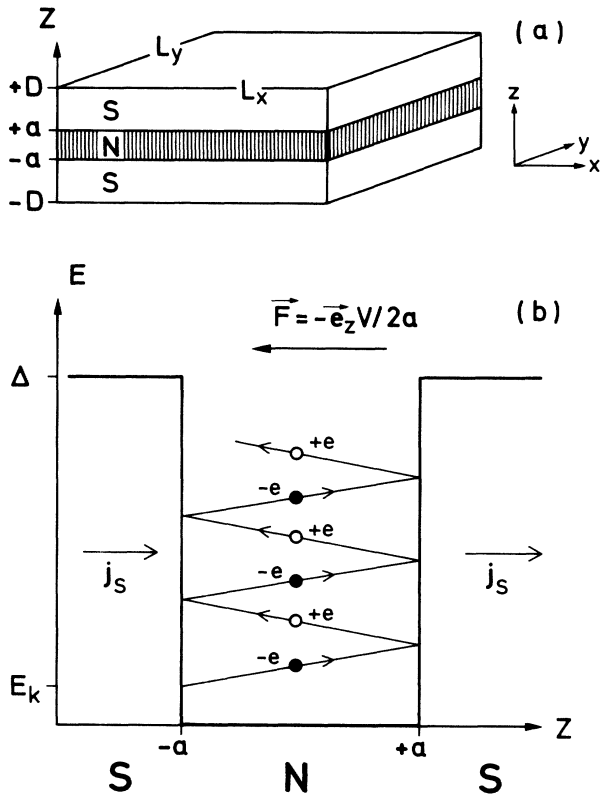

FIG. 1. (a) A weak link modeled by an *SNS* junction of normal layer thickness $2a$, total sample thickness $2D$, and cross sectional area L_xL_y. (b) Quasiparticle wave packet in the pair-potential well of an *SNS* junction gaining energy from a constant electric field F in the N layer: At time $t=0$ motion starts at energy E_k; the initial position of the wave-packet center is at $z=-b$ (with $b=a$ in the shown example). Andreev reflections change electron $(-e)$ into hole $(+e)$ wave packets and vice versa; j_s is the supercurrent density induced by Andreev reflection.

tum mechanically this acceleration process is described by the electron and hole wave-packet solutions $u_k^+(r,t)$ and $v_k^+(r,t)$ of the time-dependent BdGE (Ref. 32) given by Eqs. (2.9)–(2.18). These equations also show the wave packets u_k^- and v_k^- with momentum in negative z direction, which at time $t=0$ originate from electrons with center at $z=+b$ and E_k, and which climb down the pair-potential well. In the relaxation-time approximation one assumes, that with probability $\exp -t/T_S$ the quasiparticle is freely accelerated by the electric field until time t, where T_S is the average scattering time. The effective current carried by such a quasiparticle is proportional to the time average of the instantaneous velocity, taken between the moment when the equilibrium state is left (which one may think to be the moment when the electric field is switched on) and infinity.

The observable current density is proportional to the sum of the time averages of all (gauge-invariant) electron and hole velocities, where one has to take into account the rate $1/t_c$ at which quasiparticles start their motion from the respective initial states k. Let us assume that $2a$ is the effective length of the region where a finite electric field exists. Then the time interval between two quasiparticle "takeoffs" is

$$t_c=\begin{cases}2a/v_z, & \text{if } 2a/v_z<T_S \quad (2.1a)\\ T_S, & \text{otherwise.} \quad (2.1b)\end{cases}$$

Equation (2.1b) corresponds to the usual relaxation-time model for electrons that are freely accelerated in a (very long) normal metal until they are scattered, then return to their initial state k and begin anew their motion in the field. Equation (2.1a), on the other hand, holds in the "mesoscopic" case of ballistic transport at velocity v_z through a normal conductor of length $2a$, which is shorter than the mean free path $l=v_z/T_S$ of the electrons, and beyond whose boundaries no electric field exists: whenever an electron of velocity v_z leaves the normal conductor through one boundary another one enters it through the opposite boundary. This model conception is consistent with the Pauli principle and yields the usual Sharvin current[33] of ballistic electrons in the electric field of a contact, see Eq. (3.22). (The velocity gain in the field is assumed to be small compared to the initial velocity v_z, which is true for practically all electrons at the Fermi surface.) Thus, in computing the stationary part of the current density by averaging the quasiparticle momentum densities over a time interval $-T\le t\le +T$ with $T\to\infty$, we have to count the contributions from all the quasiparticles that at the time $t=\nu t_0$, $-T/t_0\le\nu\le+T/t_c$, have started their motion in the field from the equilibrium states k. The corresponding wave-packet functions are $u_k^{\pm}(\mathbf{r},t-\nu t_c)$ and $v_k^{\pm}(\mathbf{r},t-\nu t_c)$. Averaging also over the normal layer thickness $2a$ facilitates handling of the spatially extended wave packets. Thus, with the gauge-invariant (kinetic) momentum operator

$$\mathbf{P}=\left[\frac{\hbar}{i}\nabla+\frac{e}{c}\mathbf{A}\right] \quad (2.2)$$

and

$$e=+|e|\ ,$$

where $\mathbf{A}(z,t)$ is the vector potential related to the electric field by Eq. (A2), we obtain the time and spatially averaged current density as

$$\begin{aligned}\langle\mathbf{j}\rangle=-\frac{e}{2m}2\lim_{T\to\infty}\sum_k\sum_{\nu=-T/t_c}^{+T/t_c}\frac{1}{2T}\int_{-T}^{+T}dt\frac{1}{2a}\int_{-a}^{+a}dz\,e^{-(t-\nu t_c)/T_S}\\ \times(\{f_0(E_k)[u_k^{+*}(\mathbf{r},t-\nu t_c)\mathbf{P}u_k^+(\mathbf{r},t-\nu t_c)\\ +u_k^{-*}(\mathbf{r},t-\nu t_c)\mathbf{P}u_k^-(\mathbf{r},t-\nu t_c)]\\ +[1-f_0(E_k)][v_k^+(\mathbf{r},t-\nu t_c)\mathbf{P}v_k^{+*}(\mathbf{r},t-\nu t_c)\\ +v_k^-(\mathbf{r},t-\nu t_c)\mathbf{P}v_k^{-*}(\mathbf{r},t-\nu t_c)]\}+\text{c.c.})\ .\end{aligned} \quad (2.3)$$

Equation (2.3) is the current density in the formalism of the Bogoliubov-de Gennes equations[29,34,35] adapted to the nonstationary case of accelerated and scattered wave packets. $f_0(E_k)$ is the Fermi distribution function that gives the probability of finding a quasiparticle excitation in state k before the electric field is applied. The term independent from $f_0(E_k)$ is the contribution from the quasiparticles that are excited out of the ground state by the electric field. We do not discriminate between thermally and electrodynamically excited quasiparticles, assigning to all of them the same average inelastic-scattering time T_s. The sum over the quantum number triples k of the equilibrium eigenstates excludes the spin (which is taken into account by a factor of 2 in front of the sum). The states with opposite momenta perpendicular to the NS interfaces are treated as degenerate states[4,36] and the momentum densities of the wave packets starting out of them are given in the curly bracket by $u_k^{+*}Pu_k^+$, $v_k^+Pv_k^{+*}$ (positive z momentum) and $u_k^{-*}Pu_k^-$, $v_k^-Pv_k^{-*}$ (negative z momentum).

A quasiparticle that at the time $t=\nu t_c$ starts the acceleration process in the N layer from a state of energy E_k contributes to the time integral in Eq. (2.3) only during the time interval $\nu t_c\le t\le\nu t_c+\tau$, where $\tau=\tau(k)$ is the time after

which the quasiparticle has been accelerated to the edge of the pair-potential well and left the N layer into one of the superconducting banks. Thus, the time integral can be split into intervals of magnitude τ and the right-hand side (rhs) of Eq. (2.3) simplifies to an expression of the form

$$\frac{1}{2T}\sum_{\nu=-T/t_c}^{+T/t_c}\int_{-T}^{+T}dt\, s(t-\nu t_c)=\frac{1}{2T}\sum_{\nu=-T/t_c}^{+T/t_c}\int_{\nu t_c}^{\nu t_c+\tau}dt\, s(t-\nu t_c)$$

$$=\frac{1}{2T}\int_0^{\tau}dt' s(t')\sum_{\nu=-T/t_c}^{+T/t_c}1=\frac{1}{t_c}\int_0^{\tau}dt\, s(t)\ . \tag{2.4}$$

It is well known that to each triple k of quantum numbers there is a positive- and a negative-energy solution of the BdGE.[34] A complete set of solutions of the BdGE includes positive- and negative-energy states,[37] transitions between which are transitions between excited states and the ground state.[38] The current density does not change if instead of summing over all positive-energy states one sums over all negative-energy states[38] or adds both sums and devides by 2. It is convenient to rewrite Eq. (2.3) formally as the sum over the complete set of positive- and negative-energy eigenstates E_k. This is indicated by a caret over the summation sign:

$$\sum_k=\tfrac{1}{2}\widehat{\sum_k}\ . \tag{2.5}$$

Since electron wave functions of negative energy are identical to hole wave functions of positive energy,[34,37] see Eqs. (A24) and (A25), we thus obtain the current density in a form where the quasiparticles start their acceleration in the field with 50% probability as electrons and with 50% probability as holes, i.e., we have a true projection of the stationary electron-hole states[4] into the dynamic wave packets.

Using Eqs. (2.4) and (2.5) and defining the averaged momentum densities

$$\langle u_k^{\pm *}\mathbf{P}u_k^{\pm}\rangle=\frac{1}{2a}\frac{1}{t_c}\int_{-a}^{+a}dz\int_0^{\tau}dt\, e^{-t/T_S}u_k^{\pm *}(\mathbf{r},t)\mathbf{P}u_k^{\pm}(\mathbf{r},t)\ , \tag{2.6}$$

$$\langle v_k^{\pm}\mathbf{P}v_k^{\pm *}\rangle=\frac{1}{2a}\frac{1}{t_c}\int_{-a}^{+a}dz\int_0^{\tau}dt\, e^{-t/T_S}v_k^{\pm}(\mathbf{r},t)\mathbf{P}v_k^{\pm *}(\mathbf{r},t)\ , \tag{2.7}$$

we obtain the averaged current density in the relaxation-time approximation as

$$\langle \mathbf{j}\rangle=-\frac{e}{2m}\widehat{\sum_k}([f_0(E_k)(\langle u_k^{+*}\mathbf{P}u_k^{+}\rangle+\langle u_k^{-*}\mathbf{P}u_k^{-}\rangle)+[1-f_0(E_k)](\langle v_k^{+}\mathbf{P}v_k^{+*}\rangle+\langle v_k^{-}\mathbf{P}v_k^{-*}\rangle)]+\text{c.c.})\ . \tag{2.8}$$

The quasiparticle wave packets $u_k^{\pm}$ and $v_k^{\pm}$, which move in the electric field because of the applied voltage V, are calculated in Appendix A, where we also explain the details of the theoretical model for the potentials and fields used in the time-dependent BdGE. They define the upper and the lower component of a spinor that represents the quasiparticle wave packet in the N region:

$$\Psi_N^{\pm}(\mathbf{r},t,E_k)=\begin{bmatrix}u_k^{\pm}(\mathbf{r},t)\\ v_k^{\pm}(\mathbf{r},t)\end{bmatrix}$$

$$=\sum_{n=-\infty}^{+\infty}\left[\begin{bmatrix}1\\0\end{bmatrix}u_n^{\pm}(z,t,k)+\begin{bmatrix}0\\1\end{bmatrix}v_n^{\pm}(z,t,k)\right]e^{i\mathbf{k}_\rho\rho}\ . \tag{2.9}$$

Quasiparticle propagation parallel to the interfaces is described by

$$e^{(i\mathbf{k}_\rho\rho)},\ \mathbf{k}_\rho\rho\equiv\mathbf{e}_x k_x x+\mathbf{e}_y k_y y\ ,$$

where the spectrum of the wave vectors k_x and k_y is determined by periodic boundary conditions in x and y directions with periodicity lengths L_x and L_y.

$u_n^{\pm}$ represents the wave packet of the quasiparticle when it is an electron during the time interval between the $2n$th and $2n+1$st Andreev reflection, then it becomes a hole described by the wave packet $v_n^{\pm}$ until the next Andreev reflection, which produces an electron again, and the energy of the quasiparticle is steadily increasing (+) or decreasing (−). This can be easily seen from the explicit forms of the $u_n^{\pm}$ and $v_n^{\pm}$, which are given by equations (2.10)–(2.18):

$$u_n^+(z,t,k)=Ne^{-iE_{2n}^+t/\hbar}e^{+i(k_{2n}^+-\kappa)z}e^{i\varphi^+}\exp\left[-\left[(4na+b+z-v_{zf}t)\frac{\delta}{2\hbar v_{zf}}\right]^2\right]A_{2n}^+\left[E_k+\frac{b}{2a}eV\right], \tag{2.10}$$

$$v_n^+(z,t,k)=Ne^{-iE_{2n+1}^+t/\hbar}e^{+i(k_{2n+1}^+-\kappa)z}e^{i\psi^+}$$
$$\times\exp\left[-\left[[(4n+2)a+b-z-v_{zf}t]\frac{\delta}{2\hbar v_{zf}}\right]^2\right]A_{2n+1}^+\left[E_k+\frac{b}{2a}eV\right], \tag{2.11}$$

$$E_m^+(z)=meV+(-1)^m eV\frac{z}{2a}+E_k+eV\frac{b}{2a}, \tag{2.12}$$

$$k_m^+=k_{zf}+(-1)^m\frac{E_m^+}{\hbar v_{zf}}, \tag{2.13}$$

$$u_n^-(z,t,k)=Ne^{-iE_{2n}^-t/\hbar}e^{-i(k_{2n}^--\kappa)z}e^{i\varphi^-}\exp\left[-\left[(4na+b-z-v_{zf}t)\frac{\delta}{2\hbar v_{zf}}\right]^2\right]A_{2n}^-\left[E_k-\frac{b}{2a}eV\right], \tag{2.14}$$

$$v_n^-(z,t,k)=Ne^{-iE_{2n+1}^-t/\hbar}e^{-i(k_{2n+1}^--\kappa)z}e^{i\psi^-}$$
$$\times\exp\left[-\left[[(4n+2)a+b+z-v_{zf}t]\frac{\delta}{2\hbar v_{zf}}\right]^2\right]A_{2n+1}^-\left[E_k-\frac{b}{2a}eV\right], \tag{2.15}$$

$$E_m^-(z)=-meV+(-1)^m eV\frac{z}{2a}+E_k-eV\frac{b}{2a}, \tag{2.16}$$

$$k_m^-=k_{zf}+(-1)^m\frac{E_m^-}{\hbar v_{zf}}. \tag{2.17}$$

$\hbar k_{zf}$ is the z component of the Fermi momentum $\hbar k_F=(2m\mu)^{1/2}$. This momentum component and the corresponding velocity v_{zf} normal to the phase boundaries are related to the quasiparticle momenta $\hbar k_x$ and $\hbar k_y$ parallel to the phase boundaries by

$$k_{zf}=(k_F^2-k_x^2-k_y^2)^{1/2},\quad v_{zf}=\hbar k_{zf}/m\ ;$$
$$\kappa=eVz/4\hbar v_{zf}a\ . \tag{2.18}$$

$A_{2n}^{\pm}(E_k\pm beV/2a)$ and $A_{2n+1}^{\pm}(E_k\pm beV/2a)$, as defined by Eqs. (A32)–(A34), (A17), and (A18) are the probability amplitudes that a quasiparticle that at energy E_k starts to move as an electron against (+) or with (−) the field reappears in the N region as an electron after $2n$ Andreev reflections and as a hole after $2n+1$ Andreev reflections, respectively.

According to Eqs. (2.10)–(2.17) the $E_m^{\pm}$ and $k_m^{\pm}$ are the instantaneous local energies and momenta of the quasiparticle wave packets. This has been discussed in detail in Ref. 32 (where the notation is slightly different). Note that, because of the restriction $-a\le z\le+a$, with increasing time t the value of n increases for which the (Gaussian) wave packets are maximum. The energy parameter E_k is the starting energy of the quasiparticle at time $t=0$ and wave-packet center position at $z=\mp b$. The constant δ is the energy spread of the wave packet, see Eqs. (A35)–(A37). $\varphi^{\pm}$ and $\psi^{\pm}$ are irrelevant phase factors.

The normalization factor N is determined by the probability of finding the quasiparticle in the N region $-a<z<+a$, where the electric field exists. The dependence of this probability P_N upon $2a$, the length $D-a$ of a superconducting bank and the penetration depth $\lambda=\hbar^2k_{zf}/m(\Delta^2-E^2)^{1/2}$ of a quasiparticle of energy $E<\Delta$ into a thick bank[39] is given by

$$P_N(E)=\frac{2a}{2a+2\lambda^*} \tag{2.19}$$

with

$$\lambda^*=\begin{cases}\lambda=\dfrac{\hbar^2}{m}\dfrac{k_{zf}}{(\Delta^2-E^2)^{1/2}} & \text{for } E<\Delta,\lambda<D-a\\ D-a, & \text{otherwise.}\end{cases}$$

Supposing that for $\delta<2$ eV the condition

$$\left[\frac{4a\delta}{2\hbar v_{zf}}\right]^2\gg1 \tag{2.20}$$

is sufficiently well satisfied, the overlap of wave packet components of different n can be neglected in the normalization integral of the total wave-packet function (2.9); at a given time only one n matters so that the normalization factor becomes

$$|N|^2=\frac{1}{L_xL_y}\frac{\delta}{\sqrt{2\pi}\hbar v_{zf}}P_N\ . \tag{2.21}$$

III. WAVE-PACKET CURRENTS

We insert $u_k^{\pm}$ and $v_k^{\pm}$ as defined by Eqs. (2.9)–(2.18) into Eqs. (2.6) and (2.7) for the averaged momentum densities. A number of terms that result from the spatial derivatives cancel, and in the sum over k of the current density (2.8) the contributions from the positive and negative k_x and k_y cancel, too, Thus, the current is determined by the z-momentum densities that can be written in the form

$$\langle u_k^{\pm *} P_z u_k^{\pm} \rangle = \pm \mathbf{e}_z 2|N|^2 \sum_n \left| A_{2n}^{\pm}\left[E_k \pm \frac{b}{2a}eV\right]\right|^2 \langle\langle \hbar k_{2n}^{\pm} \rangle\rangle \ , \tag{3.1}$$

$$\langle v_k^{\pm} P_z v_k^{\pm *} \rangle = \mp \mathbf{e}_z 2|N|^2 \sum_n \left| A_{2n+1}^{\pm}\left[E_k \pm \frac{b}{2a}eV\right]\right|^2 \langle\langle \hbar k_{2n+1}^{\pm} \rangle\rangle \ , \tag{3.2}$$

where

$$\langle\langle \hbar k_{2n}^{\pm} \rangle\rangle = \frac{1}{t_c}\int_0^{\tau_l} dt\, e^{-t/T_S}\frac{1}{2a}\int_{-a}^{+a} dz\, \hbar k_{2n}^{\pm} \exp\left[-2\left[(4na+b\pm z - v_{zf}t)\frac{\delta}{2\hbar v_{zf}}\right]^2\right] \ , \tag{3.3}$$

$$\langle\langle \hbar k_{2n+1}^{\pm} \rangle\rangle = \frac{1}{t_c}\int_0^{\tau_l} dt\, e^{-t/T_S}\frac{1}{2a}\int_{-a}^{+a} dz\, \hbar k_{2n+1}^{\pm} \exp\left[-2\left[[(4n+2)a+b\mp z - v_{zf}t]\frac{\delta}{2\hbar v_{zf}}\right]^2\right] \ , \tag{3.4}$$

$$k_{2n}^{\pm} = k_e + (\pm 4na + z \pm b)\frac{eV}{2a\hbar v_{zf}} \ , \tag{3.5}$$

$$k_{2n+1}^{\pm} = k_h - [\pm(4n+2)a - z \pm b]\frac{eV}{2a\hbar v_{zf}} \ , \tag{3.6}$$

$$k_{e,h} = k_{zf} \pm \frac{E_k}{\hbar v_{zf}} \ . \tag{3.7}$$

The relative momentum change of a quasiparticle during one passage through the N region is small and the momenta vary slowly compared to the Gaussians. Therefore, the rhs of Eqs. (3.5) and (3.6) may be replaced by their values for z in the maximum of the Gaussians at $z_{e,h}^{\pm}$:

$$k_{2n}^{\pm} \approx k_e \pm \frac{eV}{2a}\frac{t}{\hbar} = k_{2n}^{\pm}(z_e^{\pm}) \ , \tag{3.8}$$

$$k_{2n+1}^{\pm} \approx k_h \mp \frac{eV}{2a}\frac{t}{\hbar} = k_{2n+1}^{\pm}(z_h^{\pm}) \ . \tag{3.9}$$

These are just the classical time changes of electron and hole momenta in the electric field $eV/2a$.

Integration of the Gaussians between $z=\pm a$ may be extended to $\pm\infty$, with the integrals being multiplied by the products of two-step functions that are nonzero only during the time intervals when the Gaussians are large for $|z|<a$, see Appendix B. One obtains

$$\frac{1}{2a}\int_{-\infty}^{+\infty} dz' \exp\left[-2\left[\frac{\delta}{2\hbar v_{zf}}\right]^2 z'^2\right] = \frac{1}{2a}\sqrt{2\pi}\frac{\hbar v_{zf}}{\delta} = \frac{1}{|N|^2}\frac{1}{\Omega_N}P_N \ , \tag{3.10}$$

where the last equality follows with Eq. (2.21); $\Omega_N = 2aL_xL_y$ is the volume of the normal conductor. The remaining time averages between $t=0$ and τ are calculated in Appendix B. With that Eqs. (3.3) and (3.4) become

$$\begin{aligned}\langle\langle \hbar k_{2n}^{\pm} \rangle\rangle = \frac{P_N}{|N|^2\Omega_N}\frac{T_S}{t_c}\Bigg\{&\left[\hbar\left[k_e \pm \frac{eV}{2a}\frac{T_s}{\hbar}\right](1-e^{-(a+b)/l}) \mp \frac{eV}{2a}\frac{a+b}{v_{zf}}e^{-(a+b)/l}\right]\delta_{n,0} \\ &+ \left[\hbar\left[k_e \pm \frac{eV}{2a}\frac{T_S}{\hbar}\right](1-e^{-2a/l}) \pm \frac{eV}{2a}\left[\frac{4na-a+b}{v_{zf}} - \frac{4na+a+b}{v_{zf}}e^{-2a/l}\right]\right] \\ &\times e^{-(4na-a+b)/l}\Theta(4na-a+b)\Bigg\} + g(\tau) \ ,\end{aligned} \tag{3.11}$$

$$\begin{aligned}\langle\langle \hbar k_{2n+1}^{\pm} \rangle\rangle = \frac{P_N}{|N|^2\Omega_N}\frac{T_S}{t_c}\Bigg[&\hbar\left[k_h \mp \frac{eV}{2a}\frac{T_S}{\hbar}\right](1-e^{-2a/l}) \\ &\mp \frac{eV}{2a}\left[\frac{4na+a+b}{v_{zf}} - \frac{4na+3a+b}{v_{zf}}e^{-2a/l}\right]\Bigg]e^{-(4na+a+b)/l}\Theta(n) + h(\tau) \ .\end{aligned} \tag{3.12}$$

Θ is the step function. The functions $h(\tau)$ and $g(\tau)$ are irrelevant, because when they are nonzero the Andreev reflection probabilities $|A_{n'}^{\pm}|^2$, n' integer, vanish so that they drop out of the momentum densities (3.1) and (3.2). The mean free path l in the exponentials, where we replace v_{zf} by its average over the Fermi surface v_z is defined as

$$l=v_z T_S \ . \tag{3.13}$$

According to Eq. (2.1),

$$T_S/t_c=(l/2a)\Theta(l/2a-1)+\Theta(1-l/2a) \ . \tag{3.14}$$

In the following, for the sake of simplicity, we present only the calculations for the clean limit $l \gg 2a$ where $\exp(-2a/l)\approx 1-2a/l$. The results for arbitrary l are given at the end of this section.

Inserting the relations (3.11) and (3.12) into the momentum densities (3.1) and (3.2) we obtain

$$\begin{aligned}\langle u_k^{\pm *} P_z u_k^{\pm}\rangle = \pm\frac{2}{\Omega_N}P_N(E_k)\sum_{n=0}^{\infty}\left|A_{2n}^{\pm}\left[E_k \pm eV\frac{b}{2a}\right]\right|^2 \\ \times\left\{\frac{a+b}{2a}\left[\hbar k_e \pm \frac{eV}{v_{zf}}\frac{a+b}{4a}\right]\delta_{n,0}+\left[\hbar k_e \pm \frac{eV}{v_{zf}}\left[2n+\frac{b}{2a}\right]\right]\right. \\ \left.\times e^{-(4na-a+b)/l}\Theta(4na-a+b)\right\}\end{aligned} \tag{3.15}$$

and

$$\langle v_k^{\pm} P_z v_k^{\pm *}\rangle = \mp\frac{2}{\Omega_N}P_N(E_k)\sum_{n=0}^{\infty}\left|A_{2n+1}^{\pm}\left[E_k \pm eV\frac{b}{2a}\right]\right|^2\left\{\left[\hbar k_h \mp \frac{eV}{v_{zf}}\left[2n+1+\frac{b}{2a}\right]\right]e^{-(4na+a+b)/l}\right\}, \tag{3.16}$$

with

$$\begin{aligned}k_e &= k_{zf}+\frac{E_k}{\hbar v_{zf}} \ , \\ k_h &= k_{zf}-\frac{E_k}{\hbar v_{zf}} \ .\end{aligned} \tag{3.17}$$

The current density (2.8), whose x and y components are zero, becomes, with Eqs. (3.15) and (3.16),

$$\begin{aligned}\langle \mathbf{j}\rangle = -\mathbf{e}_z\frac{e}{m}\frac{1}{\Omega_N}\hat{\sum_k}\sum_{n=0}^{\infty}P_N(E_k)\left\{f_0(E_k)\frac{a+b}{2a}\left[\left|A_{2n}^{+}\left[E_k+\frac{b}{2a}eV\right]\right|^2\left[\hbar k_e+\frac{eV}{v_{zf}}\frac{a+b}{4a}\right]-\left|A_{2n}^{-}\left[E_k-\frac{b}{2a}eV\right]\right|^2\right.\right. \\ \times\left[\hbar k_e-\frac{eV}{v_{zf}}\frac{a+b}{4a}\right]\delta_{n,0}+f_0(E_k)\hbar k_e e^{-(4na-a+b)/l} \\ \times\left[\left|A_{2n}^{+}\left[E_k+\frac{b}{2a}eV\right]\right|^2-\left|A_{2n}^{-}\left[E_k-\frac{b}{2a}eV\right]\right|^2\right] \\ \times\Theta(4na-a+b)-[1-f_0(E_k)]\hbar k_h e^{-(4na+a+b)/l} \\ \times\left[\left|A_{2n+1}^{+}\left[E_k+\frac{b}{2a}eV\right]\right|^2-\left|A_{2n+1}^{-}\left[E_k-\frac{b}{2a}eV\right]\right|^2\right] \\ +\left[2n+\frac{b}{2a}\right]\frac{eV}{v_{zf}}e^{-(4na-a+b)/l}\left[\left|A_{2n}^{+}\left[E_k+\frac{b}{2a}eV\right]\right|^2\right. \\ \left.\left.+\left|A_{2n}^{-}\left[E_k-\frac{b}{2a}eV\right]\right|^2\right]f_0(E_k)\Theta(4na-a+b) \\ +\left[2n+1+\frac{b}{2a}\right]\frac{eV}{v_{zf}}e^{-(4na+a+b)/l} \\ \times\left[\left|A_{2n+1}^{+}\left[E_k+\frac{b}{2a}eV\right]\right|^2+\left|A_{2n+1}^{-}\left[E_k-\frac{b}{2a}eV\right]\right|^2\right][1-f_0(E_k)]\Bigg\} \ .\end{aligned} \tag{3.18}$$

Equation (3.18) may be split into two terms:

$$\langle \mathbf{j} \rangle = \langle \mathbf{j}_N \rangle + \langle \mathbf{j}_{AR} \rangle \ , \tag{3.19}$$

$\langle j_N \rangle$ is the term proportional to $\delta_{n,0}$, which is nonzero only for $n=0$. With Eq. (A34) it becomes

$$\langle \mathbf{j}_N \rangle = -\mathbf{e}_z \frac{e^2 V}{m} \left[\frac{a+b}{2a} \right]^2 \frac{1}{\Omega_N} \hat{\sum_k} \frac{1}{v_{zf}} P_N(E_k) f_0(E_k) \ . \tag{3.20}$$

In the ohmic limit of vanishing Andreev reflection probabilities, when all terms with $n \neq 0$ are zero, $\langle j_N \rangle$ would be all that is left. In the clean limit $2a < v_z T_s$, when the "takeoff" intervals are given by $t_c = 2a/v_z$, all quasiparticles start their motion in the field at $z=-a$ or $z=+a$ so that $b=a$. The overwhelming majority of them is in continuum states above the gap that extend throughout the total junction of length $2D$ so that $P_N = 2a/2D$. We define

$$\left\langle \frac{1}{v_{zf}} \right\rangle = \frac{\hat{\sum_k} 1/v_{zf} f_0(E_k)}{\hat{\sum_k} f_0(E_k)} \equiv \frac{\alpha}{v_F}, \quad \alpha > 1 \ , \tag{3.21}$$

observe that here $P_N/\Omega_N = 1/\Omega_{SNS}$ ($\Omega_{SNS} = 2DL_xL_y$ = volume of the junction) and that the sum $\hat{\sum}_k f_0(E_k)$ over one spin and z-momentum orientation and all positive- and negative-energy states is one-fourth of the total electron number, and end up with

$$\langle \mathbf{j}_N \rangle = -\mathbf{e}_z \frac{V}{R_0 L_x L_y} \ , \qquad R_0 \equiv \frac{1}{\alpha} \frac{4p_F}{e^2 \rho} \frac{1}{L_x L_y} \ , \tag{3.22}$$

where ρ is the electron density of the junction and $p_F = (2m\mu)^{1/2}$ is the Fermi momentum. $\langle j_N \rangle$ corresponds to the Sharvin current density.[33]

In the current density due to Andreev reflections, $\langle j_{AR} \rangle$, the remaining four terms of Eq. (3.18) are combined. With the relations

$$1 - f_0(\mp|E|) = f_0(\pm|E|) \ , \tag{3.23}$$

$$k_h(\mp|E|) = k_e(\pm|E|) \ , \tag{3.24}$$

$$|A^{\pm}_{2n}(\mp|E|)|^2 = |A^{\mp}_{2n}(\pm|E|)|^2 \ , \tag{3.25}$$

$$|A^{\pm}_{2n+1}(\mp|E|)|^2 = |A^{\mp}_{2n+1}(\pm|E|)|^2 \ , \tag{3.26}$$

the $\hat{\sum}_k$ can be rewritten again as the sum $\sum_k$ over positive energies $E_k \geq 0$ only. Equations (3.25) and (3.26) result from Eqs. (A32) and (A33) in combination with Eq. (A17) for $|E| < \Delta$ and Eq. (A18) for $|E| > \Delta$ (where in the case $E < -\Delta$ the sign of the square root has to be changed). After some reordering and recasting of terms the Andreev reflection current density becomes

$$\begin{aligned}
\langle \mathbf{j}_{AR} \rangle = -\mathbf{e}_z \frac{e}{m} \frac{1}{\Omega_N} \sum_k \sum_{n=0}^{\infty} P_N(E_k) \Big\{ & \hbar \{ f_0(E_k) k_e - [1 - f_0(E_k)] k_h \} e^{-(4na - a + b)/l} \\
& \times \left[\left| A^{+}_{2n} \left[E_k + \frac{b}{2a} eV \right] \right|^2 - \left| A^{-}_{2n} \left[E_k - \frac{b}{2a} eV \right] \right|^2 \right] \Theta(4na - a + b) \\
& + \hbar [f_0(E_k) k_e - [1 - f_0(E_k)] k_h] e^{-(4na + a + b)/l} \\
& \times \left[\left| A^{+}_{2n+1} \left[E_k + \frac{b}{2a} eV \right] \right|^2 - \left| A^{-}_{2n+1} \left[E_k - \frac{b}{2a} eV \right] \right|^2 \right] \\
& + \left[2n + \frac{b}{2a} \right] \frac{eV}{v_{zf}} e^{-(4na - a + b)/l} \\
& \times \left[\left| A^{+}_{2n} \left[E_k + \frac{b}{2a} eV \right] \right|^2 + \left| A^{-}_{2n} \left[E_k - \frac{b}{2a} eV \right] \right|^2 \right] \Theta(4na - a + b) \\
& + \left[2n + 1 + \frac{b}{2a} \right] \frac{eV}{v_{zf}} e^{-(4na + a + b)/l} \\
& \times \left[\left| A^{+}_{2n+1} \left[E_k + \frac{b}{2a} eV \right] \right|^2 + \left| A^{-}_{2n+1} \left[E_k - \frac{b}{2a} eV \right] \right|^2 \right] \Big\} \ .
\end{aligned} \tag{3.27}$$

The first two terms in Eq. (3.27) contain the equilibrium momenta $\hbar k_e$ and $\hbar k_h$ of Andreev reflected electrons and holes and the last two terms are proportional to the momentum changes in the electric field. Because of condition (A4) these changes are small compared to the equilibrium momenta and their contribution to the current can be neglected. (This has been confirmed by explicit numerical computation; the E_k dependence of k_e and k_h, in fact, is negligible, too.) Thus, the current in the electric field $-\mathbf{e}_z V/2a$ is essentially due to the fact that quasiparticles with positive z-momentum components starting (with negative charge) from states below the Fermi level complete many more Andreev reflection cycles before leaving the pair-potential well than quasiparticles with negative z-momentum components.[40] [Because of Eqs. (3.25) and (3.26) $|A^{-}_{n'}(E)|^2 = |A^{+}_{n'}(-E)|^2$, n' being $2n$ or $2n+1$; the main contribution to the current

comes from the momenta $\hbar k_h$ of states below the Fermi level as can be easily seen for $T=0$ K when $f_0(E_k)=0$].

The terms with even and odd indices of the Andreev reflection probabilities can be written as one expression if we replace $2n$ by n' in the even and $2n+1$ by n' in the odd terms; then we drop the prime again: $n'\rightarrow n$. We observe that the $n=0$ terms cancel because of Eq. (A34), and end up with the final AR current density that comprises the voltage dependence only within the difference of the multiple AR probabilities:

$$\langle j_{\mathrm{AR}}\rangle=-e_z\frac{e}{m}\frac{1}{\Omega_N}\sum_k\sum_{n=1}^{\infty}P_N(E_k)\left\{\hbar\{f_0(E_k)k_e-[1-f_0(E_k)]k_h\}e^{-(2na-a+b)/l}\right.$$
$$\left.\times\left[\left|A_n^{+}\left(E_k+\frac{b}{2a}eV\right)\right|^2-\left|A_n^{-}\left[E_k-\frac{b}{2a}eV\right]\right|^2\right]\right\}. \tag{3.28}$$

The total current density for arbitrary mean free path l is found, if one multiplies $\langle j_N\rangle$ of Eq. (3.22) by the function

$$(T_S/t_c)[(a+b)/(2a)]^2(l/a)$$
$$\times[1-\exp(-2a/l)-(2a/l)\exp(-2a/l)]$$

and $\langle j_{\mathrm{AR}}\rangle$ of Eq. (3.28) by $(T_S/t_c)[1-\exp(-2a/l)]$, where, according to Eq. (3.14),

$$T_S/t_c=(l/2a)\Theta(l/2a-1)+\Theta(1-l/2a)\ . \tag{3.29}$$

IV. CURRENT-VOLTAGE CHARACTERISTICS

There are two yet undetermined parameters in the theory: the inelastic-scattering time T_S and the absolute value of the starting position, b. While T_S for quasiparticle-phonon interaction can be calculated in principle from time-dependent perturbation theory with the BdGE,[38,41] we take it here as a phenomenological parameter, estimates of which are given in Ref. 14. The position parameter b, on the other hand, has to be chosen in accordance with the relaxation-time model. When the mean free path $l=v_zT_S$ is smaller than the normal conductor length $2a$ so that a quasiparticle is scattered before it can cross the N region once, the starting position is equal to the average position where the quasiparticle appears in the N region at the beginning (and the end) of a relaxation cycle. Then the proper choice is $b=0$ for takeoff from bound states and $b=a$, if E_k belongs to the continuum states. This choice was made indiscriminately for all situations in Refs. 40 and 42. It has to be corrected for the case $l\gg 2a$ when the interval t_c between takeoffs is not T_S but $2a/v_z$ according to Eq. (2.1a). Then all quasiparticles start their motion in the field from the boundaries of the N region and $b=a$ is appropriate for all E_k.

The Andreev reflection current density of Eq. (3.28) is given by the sum over all initial states k for which there are appreciable Andreev reflection probabilities $|A_n^{\pm}|^2$ as they are defined by Eqs. (A32), (A33), (A17), and (A18). These probabilities are valid for quasiparticles with energies below the gap, if the quasiparticle completely decays in the superconducting banks, inducing a supercurrent there. This means that the quasiparticle penetration depth λ given by Eq. (2.19) has to be less than the thickness $(D-a)$ of the superconducting banks. Otherwise, there is a finite probability of electron-electron and hole-hole reflection from the outer sample surfaces that weakens $\langle j_{\mathrm{AR}}\rangle$. We take this into account in the simplest possible way by transforming $\sum_k$ into an integral over (one-fourth of) the density of all states

$$g(E)=\sum_i g_i(E)$$

and by weighting the two-dimensional density of states $g_i(E)$ of subband i by the probability $P(k_{zfi},D-a)$ of electron-hole scattering in the superconducting banks, which depends essentially only on the z component $\hbar k_{zfi}$ of the Fermi momentum in subband i at energy E, and the S layer thickness $D-a$. This filters out the effective number of states with k_{zf} appropriate for perfect Andreev reflection cycles. $P(k_{zf},D-a)$ has been calculated in Ref. 36. For small values of k_{zf} it rises from zero to a maximum close to unity in the vicinity of $k_{zf}\approx(2m\Delta/\hbar^2)^{1/2}$ and then decreases again with increasing k_{zf}. This decrease is the stronger the thinner the superconducting layers are. For thick S layers with $D-a\gg\lambda$, $P(k_{zf},D-a)$ is unity for all but the smallest k_{zf}. Thus, we define a filtered density of states $g_F(E)$ by writing in Eq. (3.28)

$$\sum_k=(\tfrac{1}{4})\int dE\sum_i g_i(E)P(k_{zfi},D-a)\equiv(\tfrac{1}{4})\int g_F(E)dE\ , \tag{4.1}$$

where the factor $\frac{1}{4}$ takes into account that only one spin and one z-momentum direction are to be considered. Energy integration goes from zero to a Bardeen-Cooper-Schrieffer (BCS) cutoff $h\omega_0$.

The quantum number triple k consists of the wave numbers k_x, k_y, and the subband index i of the energy eigenvalues $E_i(k_x,k_y)$ of the stationary BdGE for the *SNS* junction. The two-dimensional density of states $g_i(E)$ is defined as

$$g_i(E)=2(L_xL_y/4\pi^2)\int dk_x\,dk_y\,\delta(E-E_i(k_x,k_y))\ . \tag{4.2}$$

The factor of 2 counts the spin and L_xL_y is the junction area.

Quasiparticle spectra and densities of states have been computed for *SNS* junctions of various S and N layer thicknesses, where the competing effects of Andreev and surface scattering may be quite different. The details of these calculations will be presented elsewhere. Here, we

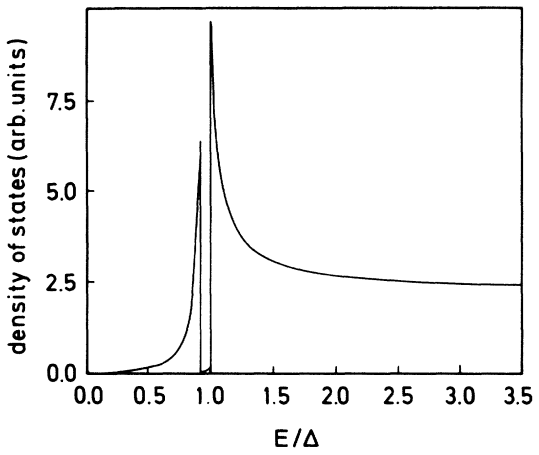

FIG. 2. Density of states $g(E)$ of an *SNS* junction with superconducting banks of thickness $D-a$ much larger than the coherence length: $D=70\,000$ Å, $a=4000$ Å. Since $P(k_{zf},D-a)=1$ in this case, $g_F(E)=g(E)$. $T_c=3.72$ K; $T=0.82\,T_c$; $k_F=1$ Å^{-1}.

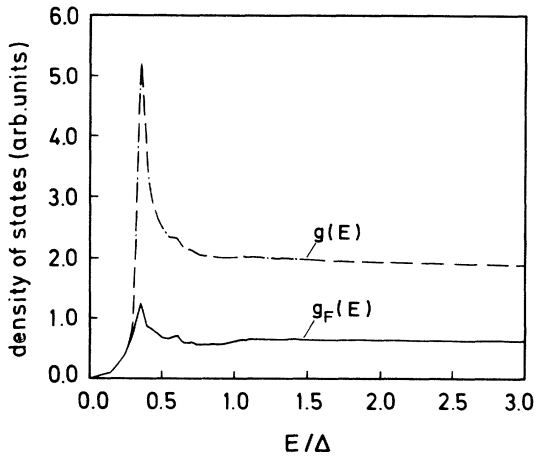

FIG. 3. Density of states $g(E)$ and filtered density of states $g_F(E)$ of an *SNS* contact with superconducting banks of thickness $D-a$ comparable to the coherence length: $D=6000$ Å; $a=4000$ Å. T_c, T, and k_F as in Fig. 2.

just report and interpret the results relevant in our context.

If the thickness $D-a$ of the superconducting banks is much larger than λ, which in turn is comparable to the BCS coherence length for practically all $E<\Delta$, the energy spectrum $E_i(k_x,k_y)$ consists of the quasicontinuum states, which can be approximated by those of a homogeneous superconductor of effective constant pair potential $\Delta[(D-a)/D]^{1/2}$,[38] and of the spatially quantized bound Andreev states that satisfy the energy eigenvalue equation

$$E_i(k_{zf})=\hbar^2 k_{zf}[i\pi+\arccos(E_i/\Delta)]/2ma\ , \qquad i=1,2,\ldots\ . \tag{4.3}$$

The corresponding total density of states $g(E)$ is shown in Fig. 2. Besides the BCS peak at $E=\Delta$ there is a subgap peak at $E<\Delta$. It results from the fact that with increasing energy and k_{zf} the $E_0(k_{zf})$ dispersion curve of the lowest subband in the spectrum of the bound Andreev states flattens out, because the quasiparticle wave functions penetrate more and more into the superconducting regions, see λ of Eq. (2.19); the lowest subband that yields the overwhelming contribution to the density of states terminates at $k_{zf}=k_F$; thus, at $E_0(k_F)$ the density of states changes abruptly to the small density from the higher subbands. With decreasing thickness $D-a$ of the S layers the BCS peak in the density of states vanishes, because the quasiparticles in the states $|E|>\Delta$ essentially "see" the N region only. If $D-a$ becomes comparable to the coherence length, the spectrum of the states with $|E|<\Delta$ still contains Andreev states at a given (low-lying) energy for sufficiently small k_{zf}. However, at the same energy but for k_{zf} so large that the quasiparticle wave functions extend into the S banks with only little damping, one has also states with the dispersion relation of a particle in a box with infinite walls at $z=\pm D$. In the situation of Fig. 3, Andreev states and "particle in a box" states accumulate in the energy range of the subgap peak in the density of states, and the peak is the consequence of this accumulation. The filtered density of states curve in Fig. 3 shows the number of the Andreev states that still originate from nearly perfect electron-hole scattering in the thin superconducting layers.

When calculating the current density $\langle j_{AR}\rangle$ by integrating over the filtered density of states one has a finite integrand only in the range of nonvanishing multiple Andreev scattering probabilities $|A_n^{\pm}|^2$. These result from the amplitudes (A32) and (A33) and Eqs. (A17) and (A18). Neglecting over-the-barrier reflections (which is quite appropriate for rounded-off pair potential edges)[43] so that

$$|\gamma(E)|^2\approx\Theta(\Delta-E)\Theta(\Delta+E)\ , \tag{4.4}$$

these probabilities can be approximated by a step-function product:

$$\left|A_n^{\pm}\left[E\pm\frac{b}{2a}eV\right]\right|^2=\prod_{\nu=1}^{n}\left|\gamma\left[E\pm\left[\nu+\frac{b}{2a}-\frac{1}{2}\right]eV\right]\right|^2$$
$$\approx\Theta\left[\Delta\pm E+\left[1+\frac{b}{a}\right]\frac{eV}{2}\right]\Theta\left[\Delta\mp E-neV+\left[1-\frac{b}{a}\right]\frac{eV}{2}\right]\ . \tag{4.5}$$

In Eq. (3.28) the terms with $[1-f_0(E_k)]k_h|A_n^-|^2$ refer to quasiparticles of *positive* z momentum that start out of the ground state, see Eqs. (3.25) and (3.26). They dominate in $\langle j_{AR}\rangle$. For them the range of integration is limited by the step functions in Eqs. (4.5) to

$$E_0 \le E \le \Delta + \left[1+\frac{b}{a}\right]\frac{eV}{2} \tag{4.6}$$

with

$$E_0 = \begin{cases} 0 \text{ for } neV - \left[1-\dfrac{b}{a}\right]\dfrac{eV}{2} - \Delta \le 0 \\ neV - \left[1-\dfrac{b}{a}\right]\dfrac{eV}{2} - \Delta \text{ otherwise.} \end{cases} \tag{4.7}$$

For a given number n of multiple Andreev reflections this integration range shrinks to zero when the voltage V approaches the value V_n defined by

$$eV_n = \frac{2\Delta}{n-1} . \tag{4.8}$$

This restriction of the possibility of multiple Andreev reflections to voltages below certain limiting values V_n is basically the physical reason for the subharmonic gap structure and the associated negative differential conductivities.[40] We will return to that in the discussion.

Numerical computation of the Andreev reflection current density (3.28) within these approximations and with the (filtered) densities of states of Figs. 2 and 3 results in total averaged current densities (3.19) that are shown by the current-voltage characteristics of Figs. 4–6. The temperature dependence of the pair potential is that of the BCS theory. The excess current is defined as the Andreev reflection current at "high" voltages $V \gg \Delta/e$. In this limit (when only one Andreev reflection is possible) Eq. (3.28) becomes

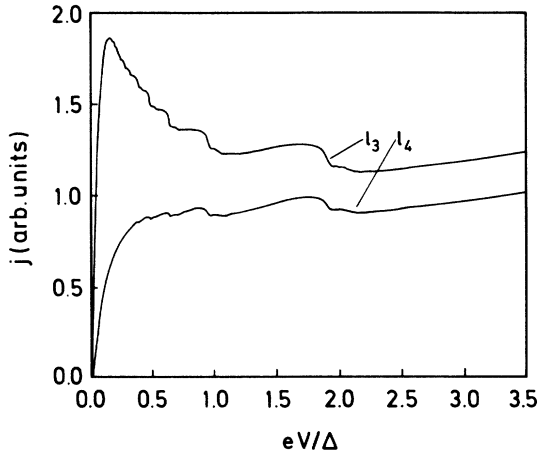

FIG. 4. Current-voltage characteristic of *SNS* junctions with thick superconducting banks, calculated with the parameters and the density of states of Fig. 2. $l_3 = 15a$; $l_4 = 5a$.

$$\langle j_{exc}\rangle \equiv \langle j_{AR}(eV \gg \Delta)\rangle = -e_z \frac{e\hbar}{4m}\frac{1}{\Omega_N} e^{-(a+b)/l} \int_{[1+(b/a)](eV/2)-\Delta}^{[1+(b/a)](eV/2)+\Delta} dE\, w(E) \tanh\left[\frac{E}{2k_BT}\right] , \tag{4.9}$$

where

$$w(E) = \sum_i k_{zfi} P(k_{zfi}, D-a) P_N(E) g_i(E) . \tag{4.10}$$

Only quasiparticles from continuum states with $|E| \approx eV$ can be pulled into the subgap region $-\Delta < E < +\Delta$ by the electric field and contribute to the excess current. In the case of a junction with thick superconducting banks their energy spectrum may be approximated by the continuous BCS spectrum of a homogeneous superconductor of pair potential Δ; furthermore $P(k_{zfi}, D-a) \approx 1$ for all (but the very smallest) k_{zfi}, and $P_N(E) = 2a/2D$. Thus, $w(E)$ becomes

$$w(E) = \frac{2a}{2D}\frac{L_xL_y}{2\pi}\frac{2m}{\hbar^2}\frac{E}{(E^2-\Delta^2)^{1/2}}\frac{2D}{\pi}k_F^2 . \tag{4.11}$$

With $b = a$ the range of integration in Eq. (4.9) is $eV - \Delta \le E \le eV + \Delta$. Within this range $\tanh(E/2k_BT)$ $[= 1 - 2f_0(E_k)]$ varies only slowly, because $eV \gg k_BT, \Delta$. Thus, it may be approximated by $\tanh(eV/2k_BT)$. The remaining integral over $E/(E^2-\Delta^2)^{1/2}$ yields 2Δ, and we obtain the excess current

$$\langle j_{exc}\rangle = -e_z (6e\rho/4p_F)\Delta \tanh(eV/2k_BT) e^{-2a/l} . \tag{4.12}$$

Here

$$\rho = \frac{k_F^3}{3\pi^2} , \qquad \frac{6e\rho}{4p_F} = \frac{6}{\alpha}\frac{1}{eR_0}\frac{1}{L_xL_y} . \tag{4.13}$$

This current density is twice as large as the one calculated in Refs. 40 and 42. The latter missed the electron-hole degeneracy of each state k in the continuum above the gap. The numerical difference between the excess current from Eqs. (4.12), (4.13), and the one from Ref. 16, i.e., $6/\alpha$ instead of $\frac{8}{3}$, is due to the average (3.21) over the Fermi surface. In addition we have the exponential dependence on the mean free path.[10]

V. DISCUSSION

A. Physical interpretation of the results

The current voltage characteristics of Figs. 4–6 show a steep rise of the current density j at low voltages for

sufficiently large mean free paths l. This is the characteristic "foot" of weak links. It is due to the large extra charge transfer associated with the very many Andreev reflections each quasiparticle undergoes before it is scattered or leaves the pair-potential well. Very many AR are possible at low voltages before a quasiparticle, which changes energy by eV between two AR, would be driven out of the pair-potential well. At very low voltages the number of Andreev reflections is essentially limited by the mean free path l and is about $n \approx l/2a$. Thus, with decreasing mean free path l this number decreases and the foot shrinks. This is clearly seen in Fig. 5. At higher voltages and large mean free paths, the number of AR within the pair-potential well becomes energy limited. It decreases as the energy gain per AR increases. Therefore, for voltages increasing from about 0.1 to 0.5 Δ/e the current decreases rapidly and the differential conductivity is negative; and for $eV > \Delta$ there is only little difference between the current-voltage characteristics for large but different mean free paths.

In the voltage range between 0.5 Δ/e and $2\Delta/e$ pronounced arches are resolved in the CVC's of Figs. 5 and 6. The nth arch extends between the voltages V_{n+1} and V_n, where, according to Eq. (4.8), $V_n = 2\Delta/(n-1)e$ is the voltage above which only $n-1$ or less AR are possible within the pair-potential well. (One AR, giving rise to the excess current, is always possible at arbitrarily high voltages V, which pull electrons from the energy range between $-eV-\Delta$ and $-eV+\Delta$ into the pair-potential well.) This is the subharmonic gap structure, and the negative-differential conductivities associated with it occur, whenever the decrease of the Andreev reflection current $\langle j_{AR} \rangle$—caused by the loss of starting states for n Andreev reflections as V approaches V_n—is stronger than the increase of the ohmic (Sharvin) current $\langle j_N \rangle$. With increasing temperature, $\langle j_{AR} \rangle$ and the SGS associated with it wither away, as it is shown by Fig. 6, because the number of thermally excited starting states increases

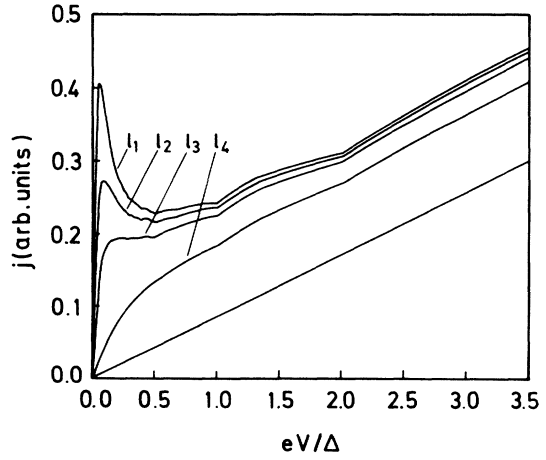

FIG. 5. Current-voltage characteristic of *SNS* junctions with thin superconducting banks and various mean free paths l in the N layer, calculated with the parameters and the filtered density of states $g_F(E)$ of Fig. 3. $l_1 = 40a$; $l_2 = 25a$; $l_3 = 15a$; $l_4 = 5a$. Also shown is the ohmic part of the current.

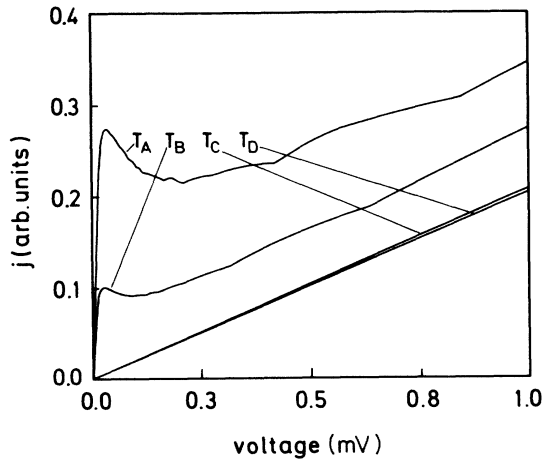

FIG. 6. Current-voltage characteristics of an *SNS* junction with thin superconducting banks, $D = 6000$ Å; $a = 4000$ Å, at various temperatures below T_c, calculated with $g_F(E)$ for $l = 25a$; $k_F \approx 1$ Å^{-1}. $T_A = 0.82\ T_c$; $T_B = 0.90\ T_c$; $T_C = 0.99\ T_c$; $T_D = T_c = 3.72$ K.

so that more and more quasiparticles with negative z momentum, "moving down" the pair-potential well, can have as many AR as quasiparticles with positive z momentum starting out of the ground state and "moving up" the well.[40] This is seen from Eq. (3.28) if one observes the symmetry relations (3.23)–(3.26) and $|A_n^-(E - beV/2a)|^2 \geq |A_n^+(E + beV/2a)|^2$.

The SGS at the V_n of Eq. (4.8) is seen so clearly in Figs. 5 and 6, because the density of the states with significant AR probability g_F has only a small peak in junctions with thin S layers, see Fig. 3. The high BCS and subgap peaks in the density of states of SNS contacts with thick S bands, on the other hand, introduce additional structures in the CVC's of Fig. 4 that somewhat obscure the $1/(n-1)$ law. The current densities are several times higher in Fig. 4 than in Figs. 5 and 6, because in the case of thick S banks practically all quasiparticles contribute to the AR current, whereas only quasiparticles with k_{zf} less than about $k_F/10$ are subject to Andreev scattering in the 2000-Å thin superconducting layers. The nearly linear increase of the sum of ohmic and excess current beyond voltages higher than about $3\Delta/e$ is the same in Figs. 4 and 5. It is determined by the (Sharvin) conductivity of Eq. (3.22).

B. Critique of the model

For vanishing voltages the condition (A37), $\delta < 2eV$, which results from wavepacket matching, becomes incompatible with the condition (2.20) for the neglect of the overlap of wave packets with different n. As V and δ approach zero the wave-packet wave functions defined by Eqs. (2.9)–(2.21) turn into the stationary solutions of the BdGE with the energy eigenvalues E_k. [In Eq. (2.9) the infinite sum of the vanishing normalization constants given by Eq. (2.21) becomes the normalization constant of the stationary waves.] Of course, the current carried by the quasiparticles in these stationary states vanishes—and in this sense our results are also valid in the limit

$V \to 0$—if the influence of a possible current bias at zero voltage is not included in the energy eigenvalues E_k. It is well known[8,34,36] that a constant ground-state current with momentum $\hbar\mathbf{q}$ per electron results in the energy spectrum

$$E_k = E_k^0 + \mathbf{p}_k \cdot \hbar\mathbf{q}/m \ , \tag{5.1}$$

where E_k^0 is the energy eigenvalue for $\mathbf{q}=0$ and $\mathbf{p}_k$ is the appropriate quasiparticle momentum in state k. In our calculations of CVC's we have used E_k^0. In order to include a zero-voltage current in the model, Eq. (3.18) has to be evaluated with E_k of Eq. (5.1) being inserted into the Fermi distribution functions[8] and Andreev scattering probabilities. This is a subject of work in progress.

The CVC's shown in Figs. 4–6 have been calculated assuming $l > 2a$. For dirty junctions with mean free paths l smaller than the N layer width the modifications indicated below Eq. (3.28) have to be taken into account in the numerical computations.

The proximity effect has been neglected. Thus, in a strict sense the theory is limited to weak links in which the normal region is several times larger than the coherence length. However, we expect qualitatively the same results for shorter N regions, because the basic physics is in the multiple Andreev reflections that are present whenever there is a spatial inhomogeneity of the pair potential.

The theory neglects possible mismatches of the Fermi velocities as they may occur in *SNS* junctions involving different materials. They give rise to normal potentials at the interfaces and a weakening of AR (Refs. 18, 20, 21, and 44) especially for larger momenta parallel to the interfaces,[19] i.e., small k_{zf}. This may be one reason why the subgap structures of the CVC's of Fig. 4 have not yet been observed in *SNS* sandwiches made from different materials, whereas the ones of Figs. 5 and 6 show all the features found experimentally in microbridges made from one material[11] (with thin superconducting surface layers where Andreev scattering is weakened for large k_{zf}).

Anisotropies of the pairing interaction[37] and the pair potential are disregarded. However, recently a generalized version of the BdGE for anisotropic and nonlocal interactions has been derived.[45] We expect that with their solutions one will be able to show in detail that the CVC's of weak links made from the high-T_c ceramic superconductors should exhibit essentially the same AR related features as one has in isotropic systems.[40]

C. Comparison with experiments

The current-voltage characteristics of variable thickness tin microbridges measured by Octavio, Skocpol, and Tinkham[11] show the foot, the subharmonic gap arches and the approach to the excess current that are also seen in Figs. 5 and 6. The relevant voltage range and the temperature dependence is that of Fig. 6. There is not the low-voltage current peak that the theory yields at low temperatures and large mean mean free paths, but rather a plateau similar to the plateau in the CVC's of Fig. 5 that corresponds to the mean free path l_3. However, the experimental plateau may also be a cut through the range of negative-differential conductivity following the initial current peak in Figs. 5 and 6 for larger mean free paths. Besides this agreement between the theoretical and experimental CVC's the sample situation in Ref. 11 corresponds to the model underlying Figs. 5 and 6 in an important detail: The normal region of the bridge is embedded in a groove in the substrate[30] and there should be only thin superconducting layers between the N region and each wall of the groove formed by the substrate. These thin S layers then grow into thick superconducting banks beyond and above the groove so that the current can flow through the junction around the edges of the groove but the quasiparticles in the active part of the junction feel essentially only the thin S layers and the hard substrate wall where they suffer normal electron-electron or hole-hole scattering for k_{zf} larger than, say, $k_F/10$. The resulting reduction of the peak of the Andreev density of states g_F as it is shown in Fig. 3, is the reason why the arches and the $1/(n-1)$ law for the subharmonic gap structure so clearly show up in Figs. 5 and 6.

In $Nb_{0.53}Ti_{0.47}/Ge$ multilayers backed by two thick (>5000 Å) superconducting Nb layers Song *et al.*[46] have observed CVC's that are similar to the l_3 curve of Fig. 5 (without the SGS arches) at $T=7.5$ K when the multilayers are normal conducting. At $T=5.7$ K, when the niobium in the multilayers is superconducting, the current decreases with increasing voltage after a low-voltage peak. In their paper the authors conclude that their essential conductance mechanism is tunneling, because they did not observe excess currents with the properties expected from the theory of Ref. 17. However, things may be different, if one does not consider the semiconducting layers as essentially insulating barriers but rather normal conductors with a small number of free carriers. Thus, the recent conjecture that the observed CVC's in superconducting-semiconducting multilayers do have something to do with multiple AR and the present theory[47] is the subject of ongoing research on the adaptation of the accelerated wave-packet formalism to superconductor–semiconductor–superconductor junctions.

Hysteresis in the low-voltage regime, indicating negative-differential conductivity, has been observed in the CVC's of Pb/Ag multilayers.[48] Weakly coupled grains of Y-Ba-Cu-O films[49] show the same effect. I-V curves of point contacts made from high-T_c superconductors also exhibit the "foot," followed by a regime of either low[50] or negative-differential conductivity.[51] In their shape the curves are similar to some of the CVC's in Figs. 4–6, and a proper choice of parameters and averaging over different magnitudes of the pair potential can even improve the qualitative agreement. However, wave-packet solutions of the generalized BdGE for superconductors with anisotropic pairing interactions will be required in order to obtain more confidence that multiple Andreev reflections are responsible for the observed CVC's of high-T_c and conventional weak links alike.

Nevertheless, despite of the necessity of further theoretical improvements the wealth of macroscopic quantum-charge-transport phenomena that are related to

the one microscopic process of electron-hole scattering by spatial variations of the pair potential, demonstrates the fundamental role of Andreev scattering in the understanding of the static and dynamic properties of inhomogeneous superconductors.[52–54]

ACKNOWLEDGMENTS

The authors gratefully acknowledge support by the Brasilian Conselho Nacional de Desenvolvimento Científico e Technológico, the Deutscher Akademischer Austauschdienst, and the Deutsche Forschungsgemeinschaft.

APPENDIX A: ACCELERATED QUASIPARTICLE WAVE PACKETS

We approximate the spatial variation of the pair potential in the *SNS* junction by the step function $\Delta\Theta(|z|-a)$: It is zero in the range $-a<z<+a$ and Δ otherwise. Plehn[43] has shown that more realistic variations of the order parameter[20,44] have relatively small influence on the density of states, whereas the probability of over-the-barrier Andreev reflections is significantly reduced. Thus, for our present purposes the widely used step-function model should be sufficient, if we disregard Andreev scattering at energies above the gap edge. We neglect the magnetic field of the current. Equal Fermi velocities in the N and S regions are assumed. This is appropriate for variable thickness microbridges consisting of the same material everywhere. Charge accumulation is supposed to occur right in the NS phase boundaries at $z=\pm a$ so that the electric field F due to the voltage V is

$$\mathbf{F}=-\mathbf{e}_z(V/2a)\Theta(a-|z|)=-c^{-1}\partial\mathbf{A}/\partial t\ . \tag{A1}$$

The vector potential

$$\mathbf{A}=-c\mathbf{F}t \tag{A2}$$

is in a gauge that makes the pair potential real and satisfies the Josephson equation for the time variation of the gauge-invariant phase difference.[32] The scalar potentials are zero. Thus, the time-dependent BdGE for electron wave function $u=u(\mathbf{r},t)$ and hole wave function $v=v(\mathbf{r},t)$ are

$$i\hbar\frac{\partial}{\partial t}u=+\left[\frac{1}{2m}\left[\mathbf{p}+\frac{e}{c}\mathbf{A}(\mathbf{r},t)\right]^2-\mu\right]u+\Delta\Theta(|z|-a)v\ , \tag{A3}$$

$$i\hbar\frac{\partial}{\partial t}v=-\left[\frac{1}{2m}\left[\mathbf{p}-\frac{e}{c}\mathbf{A}(\mathbf{r},t)\right]^2-\mu\right]v+\Delta\Theta(|z|-a)u\ ;$$

μ denotes chemical potential; $e=+|e|$. Their exact solutions involve the Airy functions. These can be expanded into a form that is just that of the electron-hole states of the junction in equilibrium for $V=0$, with the difference that energy and momentum are no longer good quantum numbers but depend on $E\pm eVz/2a$; E would be the energy eigenvalue for $V=0$.[32] The expansion is valid if

$$\frac{\hbar^2k_{zf}^2}{2m}\gg|E\pm eV|,\ \Delta\ , \tag{A4}$$

where

$$k_{zf}=(k_F^2-k_x^2-k_y^2)^{1/2};\ \mathbf{e}_xk_x+\mathbf{e}_yk_y\equiv\mathbf{k}_\rho\ . \tag{A5}$$

Defining a spinor Ψ, whose upper (lower) component is the electron (hole) wave function u (v) we can write one solution of the BdGE (A3) in the N layer $-a<z<+a$ as

$$\Psi_N(E,\mathbf{r},t)=e^{i\mathbf{k}_\rho\rho}\left[C_1^+\begin{bmatrix}1\\0\end{bmatrix}u_N^+ +C_1^-\begin{bmatrix}1\\0\end{bmatrix}u_N^- +C_2^+\begin{bmatrix}0\\1\end{bmatrix}v_N^+ +C_2^-\begin{bmatrix}0\\1\end{bmatrix}v_N^-\right] \tag{A6}$$

with

$$u_N^+=e^{-(i/\hbar)[E+eV(z/2a)]t}e^{i(k_+-\kappa)z}\ , \tag{A7}$$

$$v_N^+=e^{-(i/\hbar)[E-eV(z/2a)]t}e^{i(k_--\kappa)z}\ , \tag{A8}$$

$$u_N^-=e^{-(i/\hbar)[E+eV(z/2a)]t}e^{-i(k_+-\kappa)z}\ , \tag{A9}$$

$$v_N^-=e^{-(i/\hbar)[E-eV(z/2a)]t}e^{-i(k_--\kappa)z}\ , \tag{A10}$$

$$k_\pm=k_{zf}\pm\frac{E\pm eVz/2a}{\hbar v_{zf}}\ , \tag{A11}$$

$$\kappa=\frac{1}{2}\frac{eV}{\hbar v_{zf}}\frac{z}{2a}\ , \tag{A12}$$

$$v_{zf}=\frac{\hbar k_{zf}}{m} \tag{A13}$$

and in the superconducting banks $|z|>a$ we have

$$\Psi_S(E,\mathbf{r},t)=e^{-i(E/\hbar)t}e^{i\mathbf{k}_\rho\rho}\left[D_1^+\begin{bmatrix}1\\\gamma\end{bmatrix}e^{ik^+z}+D_1^-\begin{bmatrix}1\\\gamma\end{bmatrix}e^{-ik^+z}+D_2^+\begin{bmatrix}1\\\gamma^{-1}\end{bmatrix}e^{ik^-z}+D_2^-\begin{bmatrix}1\\\gamma^{-1}\end{bmatrix}e^{-ik^-z}\right]\ , \tag{A14}$$

$$k^\pm=\left[k_{zf}^2\pm i\frac{2m}{\hbar^2}(\Delta^2-E^2)^{1/2}\right]^{1/2}\approx k_{zf}\pm i\frac{m}{\hbar^2}\frac{(\Delta^2-E^2)^{1/2}}{k_{zf}}\quad\text{for } E<\Delta\ , \tag{A15}$$

$$k^\pm=\left[k_{zf}^2\pm\frac{2m}{\hbar^2}(E^2-\Delta^2)^{1/2}\right]^{1/2}\approx k_{zf}\pm\frac{m}{\hbar^2}\frac{(E^2-\Delta^2)^{1/2}}{k_{zf}}\quad\text{for } E>\Delta\ , \tag{A16}$$

$$\gamma=\frac{E-i(\Delta^2-E^2)^{1/2}}{\Delta}\quad\text{for } E<\Delta\ , \tag{A17}$$

$$\gamma=\frac{E-(E^2-\Delta^2)^{1/2}}{\Delta}\quad\text{for } E>\Delta\ . \tag{A18}$$

For most of the quasiparticles close to the Fermi surface the relation

$$k_{zf} > k_{zf_{\min}} = \sqrt{2m\Delta/\hbar^2} \tag{A19}$$

is true and the probability of electron-electron reflection at the interfaces is very much smaller than electron-hole scattering in the phase boundaries.[36] Thus, electrons and holes with the same direction of z momentum are coupled together by Andreev scattering and are decoupled from the electrons and holes with the opposite direction of z momentum. As a consequence the wave functions (A6) and (A14) split into the two independent solutions

$$\Psi_N^+(E,\mathbf{r},t) = e^{i\mathbf{k}_\rho\rho}\left[C_1^+\begin{bmatrix}1\\0\end{bmatrix}u_N^+ + C_2^+\begin{bmatrix}0\\1\end{bmatrix}v_N^+\right], \tag{A20}$$

$$\Psi_S^+(E,\mathbf{r},t) = e^{i\mathbf{k}_\rho\rho}e^{-i(E/\hbar)t}\left[D_1^+\begin{bmatrix}1\\\gamma\end{bmatrix}e^{ik^+z}\Theta(z-a) + D_2^+\begin{bmatrix}1\\\gamma^{-1}\end{bmatrix}e^{ik^-z}\Theta(-z-a)\right] \tag{A21}$$

and

$$\Psi_N^-(E,\mathbf{r},t) = e^{i\mathbf{k}_\rho\rho}\left[C_1^-\begin{bmatrix}1\\0\end{bmatrix}u_N^- + C_2^-\begin{bmatrix}0\\1\end{bmatrix}v_N^-\right], \tag{A22}$$

$$\Psi_S^-(E,\mathbf{r},t) = e^{i\mathbf{k}_\rho\rho}e^{-i(E/\hbar)t}\left[D_2^-\begin{bmatrix}1\\\gamma^{-1}\end{bmatrix}e^{-ik^-z}\Theta(z-a) + D_1^-\begin{bmatrix}1\\\gamma\end{bmatrix}e^{-ik^+z}\Theta(-z-a)\right], \tag{A23}$$

where the superscript $+$ ($-$) refers to positive (negative) z momentum.

The relation between the positive- and negative-energy solutions of the BdGE is

$$u^\pm(-|E|) = v^{\mp *}(+|E|), \tag{A24}$$

$$v^\pm(-|E|) = -u^{\mp *}(+|E|), \tag{A25}$$

and the most general solution of the time-dependent BdGE (A3) is the sum of all positive- and negative-energy solutions

$$\Psi_S^\pm(\mathbf{r},t) = \int_{-\infty}^{+\infty} dE\,\Psi_S^\pm(E,\mathbf{r},t), \tag{A26}$$

$$\Psi_N^\pm(\mathbf{r},t) = \int_{-\infty}^{+\infty} dE\,\Psi_N^\pm(E,\mathbf{r},t). \tag{A27}$$

Here the coefficients C and D in the wave functions (A20)–(A23) depend on E. Matching the normal region wave functions (A27) to the wave functions (A26) at the phase boundaries $\pm a$ results in the following recursion equations for the coefficients of the N-layer wave functions:[32]

$$C_1^+(E+n2eV) = C_1^+(E)\exp\left[i(4nE+4n^2eV)\frac{a}{\hbar v_{zf}}\right]A_{2n}^+(E), \tag{A28}$$

$$C_2^+(E+n2eV) = C_1^+(E-eV)\exp\left[i[(4n+2)E-eV+4n^2eV]\frac{a}{\hbar v_{zf}}\right]A_{2n+1}^+(E), \tag{A29}$$

$$C_1^-(E-n2eV) = C_1^-(E)\exp\left[i(4nE-4n^2eV)\frac{a}{\hbar v_{zf}}\right]A_{2n}^-(E), \tag{A30}$$

$$C_2^-(E-n2eV) = C_1^-(E+eV)\exp\left[i[(4n+2)E+eV-4n^2eV]\frac{a}{\hbar v_{zf}}\right]A_{2n+1}^-(E), \tag{A31}$$

with the multiple Andreev reflection probability amplitudes

$$A_{2n}^\pm(E) = \prod_{\nu=1}^{2n}\gamma\left[E\pm\nu eV\mp\frac{eV}{2}\right], \tag{A32}$$

$$A_{2n+1}^\pm(E) = \prod_{\nu=1}^{2n+1}\gamma\left[E\pm\nu eV\mp\frac{eV}{2}\right] = \gamma\left[E\pm 2neV\pm\frac{eV}{2}\right]A_{2n}^\pm(E), \tag{A33}$$

and

$$A_0^\pm(E) = 1. \tag{A34}$$

$|\gamma(\varepsilon)|^2$ is the probability that an Andreev reflection occurs at energy ε in the phase boundary of a semi-infinite superconducting bank. According to Eq. (A17) it is unity for $E<\Delta$. For $E>\Delta$ it decreases rapidly with E and may be approximate by zero for self-consistent pair potentials with rounded-off edges.[43]

Because of the recursion relations (A28)–(A31) the coefficients $C_2^\pm$ are completely determined by the

coefficients $C_1^{\pm}$ that in turn can be chosen freely only within an energy interval of width $2eV$. We choose a Gaussian spectral density

$$C_1^{\pm}(E)=\frac{N}{\sqrt{\pi\delta^2}}e^{-[(E-\gamma_k)/\delta]^2}e^{i(E/\hbar v_{zf})b}\ , \tag{A35}$$

with

$$n_k 2eV \le \gamma_k \le (n_k+1)2eV\ , \tag{A36}$$

n_k integer and

$$\delta^2 < (2eV)^2\ . \tag{A37}$$

This defines the wave packet of a quasiparticle that starts its motion in the field from state k at position $z=-b$; γ_k is the wave-packet energy in the center of the N-layer before the first Andreev reflection occurs, see Eqs. (A43), (2.12), and (2.16); $b \le a$. Since equilibrium states with positive and negative z momenta are degenerate, we choose the same initial energy distribution (A35) for wave packets with opposite momenta. The inequality (A37) makes sure that the amplitude of $C_1^{\pm}(E)$ is small outside the interval (A36). With the help of the recursion equations (A28)–(A31) we can split the integral of Eq. (A27) into energy intervals of width $2eV$ and relate these intervals to the initial one defined by Eq. (A36). This results in the normal-layer wave function

$$\Psi_N^{\pm}(\mathbf{r},t,E_k)=\begin{bmatrix}u_k^{\pm}(\mathbf{r},t)\\ v_k^{\pm}(\mathbf{r},t)\end{bmatrix}=\sum_{n=-\infty}^{+\infty}\left[\begin{bmatrix}1\\0\end{bmatrix}u_n^{\pm}(z,t,k)+\begin{bmatrix}0\\1\end{bmatrix}v_n^{\pm}(z,t,k)\right]e^{i\mathbf{k}_\rho\rho}\ , \tag{A38}$$

with

$$u_n^{+}(z,t,k)=\int_{n_k 2eV}^{(n_k+1)2eV}dE\ C_1^{+}(E+n2eV)u_N^{+}(E+n2eV)\ , \tag{A39}$$

$$v_n^{+}(z,t,k)=\int_{n_k 2eV+eV}^{(n_k+1)2eV+eV}dE\ C_2^{+}(E+n2eV)v_N^{+}(E+n2eV)\ , \tag{A40}$$

and

$$u_n^{-}(z,t,k)=\int_{n_k 2eV}^{(n_k+1)2eV}dE\ C_1^{-}(E-n2eV)u_N^{-}(E-n2eV)\ , \tag{A41}$$

$$v_n^{-}(z,t,k)=\int_{n_k 2eV-eV}^{(n_k+1)2eV-eV}dE\ C_2^{-}(E-n2eV)v_N^{-}(E-n2eV)\ . \tag{A42}$$

In Eq. (A38) summation over n formally runs to $-\infty$ because integration over E in Eqs. (A26) and (A27) does. However, u_n and v_n are vanishingly small for $n<0$.

We evaluate the integrals (A39)–(A42) with the help of Eqs. (A7)–(A10) (where E is replaced by $E\pm 2neV$), the relations (A28)–(A34) and the Gaussian (A35). With the definition

$$\gamma_k \equiv E_k \pm eV\frac{b}{2a}\ , \tag{A43}$$

this results in Eqs. (2.10)–(2.17).

APPENDIX B: TIME INTEGRATION IN THE AVERAGED MOMENTUM DENSITIES

We combine Eq. (3.10), multiplied by the appropriate step functions, with Eqs. (3.3) and (3.4) and get

$$\langle\langle \hbar k_{2n}^{\pm} \rangle\rangle=\frac{P_N}{|N|^2\Omega_N}\frac{1}{t_c}\int_0^{\tau}dt\ e^{-t/T_S}\hbar\left[k_e\pm\frac{eV}{2a}\frac{t}{\hbar}\right]\Theta(4na+a+b-v_{zf}t)\Theta(a-4na-b+v_{zf}t)\ , \tag{B1}$$

$$\langle\langle \hbar k_{2n+1}^{\pm} \rangle\rangle=\frac{P_N}{|N|^2\Omega_N}\frac{1}{t_c}\int_0^{\tau}dt\ e^{-t/T_S}\hbar\left[k_h\mp\frac{eV}{2a}\frac{t}{\hbar}\right]$$
$$\times\Theta((4n+2)a+a+b-v_{zf}t)\Theta(a-(4n+2)a-b+v_{zf}t)\ . \tag{B2}$$

The limits for time intergration in (B1) and (B2) are given by

$$4na-a+b \le v_{zf}t \le 4na+a+b \tag{B3}$$

and

$$(4n+2)a-a+b \le v_{zf}t \le (4n+2)a+a+b\ , \tag{B4}$$

respectively. Thus, the time integrals may be split into intervals:

$$I^{\pm}_{2n}(0,\tau)\equiv\int_0^{\tau}dt\,e^{-t/T_S}\hbar\left[k_e\pm\frac{eV}{2a}\frac{t}{\hbar}\right]\Theta(4na+a+b-v_{zf}t)\Theta(a-4na-b+v_{zf}t) \tag{B5}$$

$$=I^{\pm}_{2n}\left[0,\frac{a+b}{v_{zf}}\right]\delta_{n,0}+I^{\pm}_{2n}\left[\frac{4na-a+b}{v_{zf}},\frac{4na+a+b}{v_{zf}}\right][\Theta(4na-a+b)\Theta(v_{zf}\tau-4na-a-b)]$$

$$+I^{\pm}_{2n}\left[\frac{4na-a+b}{v_{zf}},\tau\right][\Theta(v_{zf}\tau-4na+a-b)\Theta(4na+a+b-v_{zf}\tau)]\,, \tag{B6}$$

$$I^{\pm}_{2n+1}(0,\tau)\equiv\int_0^{\tau}dt\,e^{-t/T_S}\hbar\left[k_h\mp\frac{eV}{2a}\frac{t}{\hbar}\right]\Theta((4n+2)a+a+b-v_{zf}t)\Theta(a-(4n+2)a-b+v_{zf}t) \tag{B7}$$

$$=I^{\pm}_{2n+1}\left[\frac{(4n+2)a-a+b}{v_{zf}},\frac{(4n+2)a+a+b}{v_{zf}}\right][\Theta(n)\Theta(v_{zf}\tau-(4n+2)a-a-b)]$$

$$+I^{\pm}_{2n+1}\left[\frac{(4n+2)a-a+b}{v_{zf}},\tau\right][\Theta(v_{zf}\tau-(4n+2)a+a-b)\Theta((4n+2)a+a-b-v_{zf}\tau)]\,. \tag{B8}$$

The integrals defined by Eqs. (B5) and (B7) have the solutions

$$I^{\pm}_{2n}(t_i,t_f)=\hbar\left[k_e\pm\frac{eV}{2a}\frac{T_S}{\hbar}\right]T_S(e^{-t_i/T_S}-e^{-t_f/T_S})\pm\frac{eV}{2a}T_S(t_ie^{-t_i/T_S}-t_fe^{-t_f/T_S})\,, \tag{B9}$$

$$I^{\pm}_{2n+1}(t_i,t_f)=\hbar\left[k_h\mp\frac{eV}{2a}\frac{T_S}{\hbar}\right]T_S(e^{-t_i/T_S}-e^{-t_f/T_S})\mp\frac{eV}{2a}T_S(t_ie^{-t_i/T_S}-t_fe^{-t_f/T_S})\,. \tag{B10}$$

Inserting these results into Eqs. (B1) and (B2) we arrive at Eqs. (3.11) and (3.12). The neglect of the functions $g(\tau)$ and $h(\tau)$ corresponds to $\tau\rightarrow\infty$ in Eqs. (B6) and (B8).

[1] A. L. de Lozanne and M. R. Beasely, in *Nonequilibrium Superconductivity*, edited by D. N. Langenberg and A. I. Larkin (North-Holland, Amsterdam, 1986).

[2] K. K. Likharev, Rev. Mod. Phys. **51**, 101 (1979).

[3] A. F. Andreev, Zh. Eksp. Teor. Fiz. **46**, 1823 (1964) [Sov. Phys. JETP **19**, 1228 (1964)].

[4] A. F. Andreev, Zh. Eksp. Teor. Fiz. **49**, 655 (1965) [Sov. Phys. JETP **22**, 455 (1966)].

[5] W. L. McMillan and P. W. Anderson, Phys. Rev. Lett. **16**, 85 (1966).

[6] W. J. Tomasch and T. Wolfram, Phys. Rev. Lett. **16**, 352 (1966).

[7] C. Ishii, Prog. Theor. Phys. **44**, 1525 (1970).

[8] J. Bardeen and J. L. Johnson, Phys. Rev. B **5**, 72 (1972).

[9] A. V. Svidzinsky, T. N. Antsygina, and E. N. Bratus, J. Low. Temp. Phys. **10**, 131 (1973).

[10] I. O. Kulik and Yu. N. Mitsai, Fiz. Nizk. Temp. **1**, 906 (1975) [Sov. J. Low Temp. Phys. **1**, 434 (1975)].

[11] M. Octavio, W. J. Skocpol, and M. Tinkham, Phys. Rev. B **17**, 159 (1978).

[12] L. G. Aslamazov and A. I. Larkin, Zh. Eksp. Teor. Fiz. **70**, 1340 (1976) [Sov. Phys. JETP **43**, 698 (1976)].

[13] A. A. Golub, Zh. Eksp. Teor. Fiz. **7**, 341 (1976) [Sov. Phys. JETP **44**, 178 (1976)].

[14] A. Schmid, G. Schön, and M. Tinkham, Phys. Rev. B **21**, 5076 (1980).

[15] S. N. Artemenko, A. F. Volkov and A. V. Zaitsev, Zh. Eksp. Teor. Fiz. **76**, 1816 (1979) [Sov. Phys. JETP **49**, 924 (1979)].

[16] T. M. Klapwijk, G. E. Blonder, and M. Tinkham, Physica B+C **109&110B**, 1657 (1982).

[17] G. E. Blonder, M. Tinkham, and T. M. Klapwijk, Phys. Rev. B **25**, 4515 (1982).

[18] M. Octavio, M. Tinkham, G. E. Blonder, and T. M. Klapwijk, Phys. Rev. B **27**, 6739 (1983).

[19] M. Yu. Kupriyanov, Fiz. Nizk. Temp. **7**, 700 (1981) [Sov. J. Low Temp. Phys. **7**, 342 (1981)].

[20] A. D. Zaikin, in *Nonequilibrium Superconductivity*, edited by V. L. Ginzburg (Nova Science, Commack, 1988), pp. 57–136.

[21] R. Hoonsawat and I. M. Tang, Phys. Lett. A **127**, 441 (1988).

[22] M. A. Peshkin and R. A. Buhrman, Phys. Rev. B **28**, 161 (1983).

[23] A. Hahn, Phys. Rev. B **31**, 2816 (1985).

[24] A. Hahn, Jpn. J. Appl. Phys. **26**, Suppl. **26-3**, 1599 (1987).

[25] L. Kramer and A. Baratoff, Phys. Rev. Lett. **38**, 518 (1977).

[26] L. Kramer and R. J. Watts-Tobin, Phys. Rev. Lett. **40**, 1041 (1978).

[27] L. P. Gor'kov and G. M. Eliashberg, Zh. Eksp. Teor. Fiz. **54**, 612 (1968) [Sov. Phys. JETP **27**, 328 (1968)].

[28] G. Schön and V. Ambegaokar, Phys. Rev. B **19**, 3515 (1979).

[29] R. Kümmel, Z. Phys. **218**, 472 (1969).

[30] M. Octavio (unpublished).

[31] W. Klein, R. P. Huebener, S. Gauss, and J. Parisi, J. Low Temp. Phys. **61**, 413 (1985).

[32] R. Kümmel and W. Senftinger, Z. Phys. B **59**, 275 (1985).

[33] Y. V. Sharvin, Zh. Eksp. Teor. Fiz. **48**, 984 (1965) [Sov. Phys. JETP **21**, 655 (1965)].

[34]P. G. de Gennes, *Superconductivity of Metals and Alloys* (Benjamin, New York, 1966).
[35]J. Bardeen, R. Kümmel, A. E. Jacobs, and L. Tewordt, Phys. Rev. **187**, 556 (1969).
[36]R. Kümmel, Phys. Rev. B **16**, 1979 (1977); there is a typographical error in Eq. (B3) for $P(k_{zf},D-a)$: in the numerator the term in the first curly bracket has to be squared.
[37]W. N. Mathews, Jr., Phys. Status Solidi B **90**, 327 (1978).
[38]V. Nino and R. Kümmel, Phys. Rev. B **29**, 3957 (1984).
[39]I. Batoulis and R. Kümmel, Z. Phys. B **62**, 451 (1986).
[40]R. Kümmel, B. Huckestein, and R. Nicolsky, Solid State Commun. **65**, 1567 (1988).
[41]H. Aberle and R. Kümmel, Phys. Rev. Lett. **57**, 3206 (1986).
[42]R. Kümmel, B. Huckestein, and R. Nicolsky, Jpn. J. Appl. Phys. **26**, Suppl. **26-3**, 1471 (1987).
[43]H. Plehn (private communication).
[44]G. Kieselmann, Phys. Rev. B **35**, 6762 (1987).
[45]O. Wacker, Diplomarbeit, Universität Würzburg, 1989 (unpublished).
[46]S. N. Song, B. Y. Jin, F. L. Du, and J. B. Ketterson, Superlatt. Microstruct. **3**, 485 (1987).
[47]S. N. Song (private communication).
[48]H. C. Yang, C. H. Nien, H. H. Sung, and C. H. Chen, J. Low Temp. Phys. **75**, 243 (1989).
[49]J. Mannhart, P. Chaudhari, D. Dimos, C. C. Tsuei, and T. R. McGuire, Phys. Rev. Lett. **21**, 2476 (1988).
[50]A. Th. A. M. de Waele *et al.*, Phys. Rev. B **35**, 8858 (1987).
[51]P. Leiderer, R. Feile, B. Renker, and D. Ewert, Z. Phys. B **67**, 25 (1987).
[52]S. Strässler and P. Wyder, Phys. Rev. Lett. **10**, 225 (1963).
[53]P. A. M. Benistant, H. van Kempen, and P. Wyder, Phys. Rev. Lett. **51**, 817 (1983).
[54]W. Zhang, J. Kurkijärvi, D. Rainer, and E. V. Thuneberg, Jpn. J. Appl. Phys. **26**, Suppl. **26-3**, 137 (1987).